

# Contributions of microstructure and chemical composition to the mechanical properties of dentin

H. Ryou · N. Amin · A. Ross · N. Eidelman ·  
D. H. Wang · E. Romberg · D. Arola

Received: 30 January 2011 / Accepted: 14 March 2011 / Published online: 1 April 2011  
© Springer Science+Business Media, LLC 2011

**Abstract** The influence of microstructural variations and chemical composition to the mechanical properties and apparent flaw sensitivity of dentin were evaluated. Rectangular beams ( $N = 80$ ) of the deep and superficial coronal dentin were prepared from virgin 3rd molars; twenty beams of each region were nominally flaw free and the remainder possessed a single “surface flaw” via a Vickers indentation. Mechanical properties were estimated in four-point flexure and examined using Weibull statistics. Fourier Transform Infrared Microspectroscopy in Reflectance Mode (FTIR-RM) was used to quantify the relative mineral

to collagen ratios. Results showed that the average flexural strength, and strain and energy to fracture of the deep dentin beams were significantly lower ( $P < 0.005$ ) than for the superficial dentin. While the deep dentin exhibited the highest mineral/collagen ratio and lowest damage tolerance, there was no significant effect of the surface flaws. Weibull analyses suggest that deep dentin possesses a larger distribution of intrinsic flaw sizes that contributes to the location dependence in strength.

**Keywords** Damage · Dentin · FTIR microspectroscopy · Fracture · Strength

Support for the following investigation was provided by the National Institutes of Health (NIDCR R01DE016904) and the National Science Foundation (BES 0238237).

H. Ryou · N. Amin · A. Ross · D. Arola (✉)  
Department of Mechanical Engineering, University of Maryland  
Baltimore County, 1000 Hilltop Circle, Baltimore,  
MD 21250, USA  
e-mail: darola@umbc.edu

N. Eidelman  
Paffenbarger Research Center, American Dental Association  
Foundation, National Institutes of Standards and Technology,  
Gaithersburg, MD 20899, USA

D. H. Wang  
School of Mechanical Engineering and Automation, Kyungnam  
University, 631-791 Masan, South Korea

E. Romberg  
Department of Health Promotion and Policy, Baltimore College  
of Dental Surgery, University of Maryland, Baltimore,  
MD 21201, USA

D. Arola  
Department of Endodontics, Prosthodontics, and Operative  
Dentistry, Baltimore College of Dental Surgery, University  
of Maryland, Baltimore, MD 21201, USA

## 1 Introduction

Restorative dentistry is largely comprised of identifying and removing tooth tissues that have been undermined by bacterial plaque. The excavation of enamel and dentin is performed to remove demineralized tissue, while balancing concerns related to prevention and conservation. There are other relevant concerns, including the time required for introducing the required cavity preparation and the potential for patient discomfort. These factors are potentially related to the rate of material removal, which is also important in the machining of engineering materials. For engineering materials the potential for introducing near-surface damage and/or strength-limiting flaws is an equal or greater concern. Defects introduced during machining/grinding of brittle materials are detrimental, and are often the primary cause for reduction of strength [e.g. 1–4]. As such, the introduction of damage within dentin or enamel during the cavity preparation could be equally deleterious.

Sehy and Drummond [5] introduced Class I or Class II MOD preparations in molars using either a high speed

handpiece with coarse diamond bur or Er:YAG laser. The preparation was followed by placement of a resin composite, bulk curing to maximize interfacial stresses, and evaluation of the tooth-composite interface using scanning electron microscopy. Neither method of preparation was found to result in significant evidence of microcracking in dentin. But two more recent studies reported that flaws introduced within dentin during material removal processes served as the origin of fracture [6] and caused significant reductions in strength [7]. In fact, cracks exceeding 100  $\mu\text{m}$  in length were introduced within the dentin under some conditions of laser treatment [7]. Flaws introduced during the restorative process are expected to be too small to cause tooth fracture under the stresses developed within these teeth during oral function. But dentin is susceptible to fatigue [8–10] and small (i.e. non-critical) flaws may undergo cyclic extension via fatigue crack growth until reaching a critical length that enables fracture of the tooth [8, 11]. Evidence of fatigue crack growth has been identified in restored teeth [12]. The probability of introducing detrimental flaws/cracks during a cavity preparation may be a function of the local microstructure and its influence on the mechanical behavior.

The “flaw sensitivity” of a material describes the potential for flaws to serve as the cause of failure under load-bearing conditions. This quality can be assessed by the reduction in strength incurred by the presence of known flaws, or by the statistical distribution of failures. Past studies have recommended that the properties of dentin should be assessed according to a damage mechanics approach, which accounts for the distribution of intrinsic flaws [13, 14]. However, the flaw sensitivity of hard tissues has received limited attention. The primary objective of this study was to evaluate the mechanical behavior of coronal dentin and to assess the importance of microstructure and chemical composition on the apparent flaw sensitivity of the tissue.

## 2 Materials and methods

Caries free third molars from a group of young individuals ( $17 \leq \text{age} \leq 27$ ) were obtained from participating dental practices in Maryland according to a protocol approved by the Institutional Review Board of the University of Maryland Baltimore County. The extracted teeth were maintained in Hanks Balanced Salt Solution (HBSS) with 0.2% sodium azide at 4°C, then cast in a polyester resin foundation and sectioned using a programmable slicer/grinder<sup>1</sup> and diamond impregnated slicing wheels (#320 mesh abrasives) under a continuous water-based coolant

bath. Primary sections were made in the bucco-lingual plane, and secondary sectioning was performed to obtain rectangular beams with dentin tubules aligned perpendicular to the length (Fig. 1a) and with geometry as shown in Fig. 1b. The beam cross-section was produced within  $\pm 0.01$  mm of the target dimensions, which is important to the volume and surface area of the beams and the corresponding flaw population. The average surface roughness (Ra) resulting from sectioning was assessed using contact profilometry and was less than 0.2  $\mu\text{m}$ . A total of 80 beams were prepared using these methods from approximately 40 different molars.

The groups of deep and superficial dentin (40 beams each) were further subdivided into two balanced groups ( $N = 20$ ), one of which was regarded as the nominally “flaw-free” control and the second modified by the introduction of a well-defined surface flaw. Specifically, an indent was introduced on the tensile side of selected beams using a commercial microhardness tester<sup>2</sup> and Vickers diamond indenter with load of 0.25 kg and duration of 15 s. A single indent was introduced within 20 beams each of deep and superficial dentin (40 total). The indentation diagonals were oriented parallel and perpendicular to the beam length (Fig. 1b). For the deep dentin beams the average indentation diagonal length ( $d$ ) and depth ( $t$ ) were 175 and 35.4  $\mu\text{m}$ , respectively. The indent depth is known directly from the Vickers indenter geometry (136° included angle). In superficial dentin the average  $d$  and  $t$  were 172 and 34.7  $\mu\text{m}$ , respectively, and not significantly different ( $P > 0.05$ ). Note that this method is similar to the fracture toughness of engineering ceramics [15] and has been adopted for evaluating dental ceramics as well [e.g. 16]. But in contrast to the SCF method, the indent was not expected to cause development of a crack in dentin. Here the indent was expected to promote a stress concentration that competed with the intrinsic flaws as the origin of failure. Using the indentation diagonal and depth, the stress concentration promoted under flexure was approximately 1.75 [17].

All of the dentin specimens were loaded within a bath of HBSS bath (22°C) under four-point flexure to failure using a universal testing system.<sup>3</sup> Loading was performed at a cross-head rate of 0.1 mm/min under displacement control according to the flexure arrangement in Fig. 1b; the beams were oriented with tubules aligned in the direction of loading (perpendicular to the beam length). Beams with indents were tested such that the indented surface was subjected to tension. The instantaneous load and load-line displacement were monitored at a frequency of 2 Hz to

<sup>1</sup> K.O. Lee Model S3818EL, Aberdeen, SD.

<sup>2</sup> HMV 2000, Micro Hardness Tester, Shimadzu, Nakagyo-ku, Kyoto, Japan.

<sup>3</sup> EnduraTEC Model ELF 3200, Minnetonka, MN.

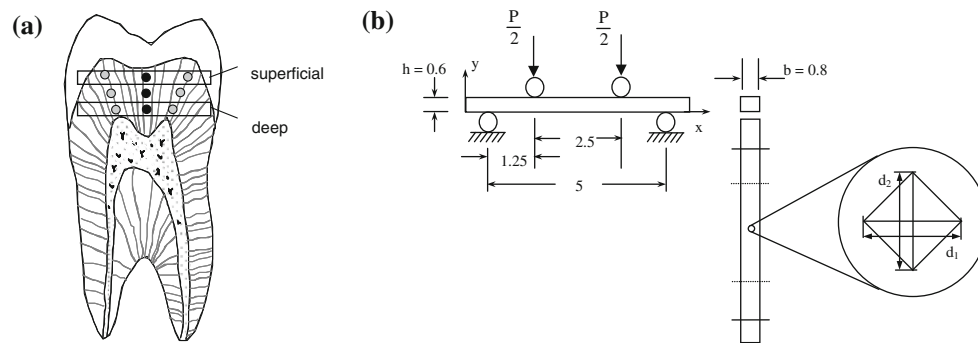


**Fig. 1** Schematic diagram of the beams, tubule orientation and flexure loading geometry. **a** An outline of the regions selected in obtaining the beams for the flexure analysis. The *grey* and *black* circles represent the relative locations in the cuspal and the intercuspal regions, respectively, where the FTIR-RM spectra were

failure. The flexure stress was estimated according to conventional beam theory from the load and measured beam geometry, whereas the actuator displacement was used with the loading geometry to determine the strain distribution. A calibration was used using aluminum and steel beams to account for the machine compliance in the assessment of strain. Stress–strain diagrams were constructed from the estimated flexure stress and strain at the beam surface. The elastic modulus of the specimens was determined from the tangent response up to 0.2% strain, and both the strength and strain to fracture were determined directly from the diagrams. Also, the energy to fracture (in flexure) was evaluated from the total area under the stress–strain curves as described earlier [9, 10]. Statistical distributions in strength, critical strain and energy to fracture were evaluated using the 2-parameter Weibull distribution [18] where the dependent variable (e.g. strength) was described according to the Weibull modulus and characteristic value. These parameters were estimated using both least squares error and maximum likelihood estimation due to differences in the Weibull modulus obtained using these two approaches [19]. Fracture surfaces of the beams were analyzed using both optical and electron microscopy. Those beams examined using the Scanning Electron Microscope (SEM)<sup>4</sup> were sputtered with gold–palladium and evaluated in the Secondary Electron Imaging (SEI) mode.

Spatial variations in the mineral to organic matrix ratios and the relative organic content of the dentin were examined using Fourier Transform Infrared microspectroscopy in Reflectance Mode (FTIR-RM). The suitability of FTIR-RM to map dentin and to determine its properties in a position resolved fashion was established previously [20]. Briefly, five additional 3rd molars within the aforementioned age range were sectioned bucco-lingually and

quantified. Similar to description of the beams, the locations of analysis consisted of deep, middle and superficial coronal dentin. **b** Nominal specimen geometry and flexure loading configuration. For those with an indent, the indented surface was loaded in tension (bottom of the beam and within the interior two loading pins)

mounted within cold-cure epoxy (Epofix HQ resin and hardener, Struers) with the sectioned surface oriented outwards. The sectioned surfaces were dry polished using silicon carbide abrasive papers sequentially down to 4000 grit, and then finished using diamond particle suspensions (9, 3 and 0.04  $\mu\text{m}$  particle diameters). After polishing the specimens were wax mounted on glass slides and their polished surfaces were leveled parallel to the slide. The evaluation was performed using an FTIR microscope<sup>5</sup> interfaced with a spectrophotometer<sup>6</sup> described previously [21]. FTIR-RM maps were obtained over the entire sectioned surfaces in a grid pattern with spatial resolution of  $90 \times 90 \mu\text{m}^2$  spot size in the  $650$  to  $4000 \text{ cm}^{-1}$  region with  $8 \text{ cm}^{-1}$  spectral resolution and 16 scans per spectrum. The reflectance spectra were transformed to absorbance spectra using the Kramers–Kronig transformation algorithm [22] for dispersion correction. The FTIR-RM maps were processed as mineral and protein (i.e. collagen) maps [(identified from the area under the  $\nu_3\text{PO}_4$  peaks at  $(980\text{--}1200) \text{ cm}^{-1}$  and under the amide I peak at  $(1595\text{--}1720) \text{ cm}^{-1}$  spectral regions, respectively)]. Both the dispersion and baseline corrected maps of each tooth were processed using commercial software<sup>7</sup> and the areas of the  $\nu_3\text{PO}_4$  and amide I peaks were calculated [21] and used to quantify the mineral to collagen ratios and the relative collagen contents. These measures were obtained along the cuspal axes and within the intercuspal region at three depths from the DEJ (Fig. 1a). The inner and outer evaluation areas corresponded to deep and superficial dentin, respectively. Within all nine regions (3 depths and 3 paths) the spectral information was averaged over a  $4 \times 4$  grid of the  $90 \times 90 \mu\text{m}^2$  windows (effective area of  $0.13 \text{ mm}^2$ ). Differences in the average spectral information

<sup>5</sup> Nic-Plan, Nicolet Instrumentations Inc. Madison, WI.

<sup>6</sup> Magna-IR 550, Nicolet Instrumentations Inc. Madison, WI.

<sup>7</sup> ISys software package (Spectral Dimensions Inc., Olney, MD).

<sup>4</sup> Jeol JSM 5600, Peabody, MA.

between the cuspal and intercuspal regions and at the three depths were evaluated using a one-way ANOVA. Differences in the flexural properties between the deep and superficial dentin and between beams with and without indents were also compared. Significance was defined by  $P \leq 0.05$ .

### 3 Results

Typical stress strain diagrams for deep and superficial dentin beams are shown in Fig. 2. In general, the responses exhibited a distinct linear-elastic region with a small degree of nonlinear inelastic behavior just prior to failure. The average mechanical properties for the four specimen groups are listed in Table 1. Superficial dentin exhibited a significantly higher elastic modulus, ultimate flexure strength, critical strain and energy to fracture than the deep dentin. The largest differences in mechanical behavior were found in the strength and energy to fracture, which were over 50 and 100% greater in the superficial dentin, respectively. There was no significant difference ( $P > 0.05$ ) in the properties between beams with and without surface flaws at either of the two depths.

Weibull distributions for the strength of the dentin beams are shown in Fig. 3. Specifically, the distribution in strength for specimens without flaws (control) and those with flaws are shown in Fig. 3a and b, respectively. The corresponding Weibull parameters for the estimated strength are listed in Table 2 along with values for the strain to fracture. There were no significant differences in

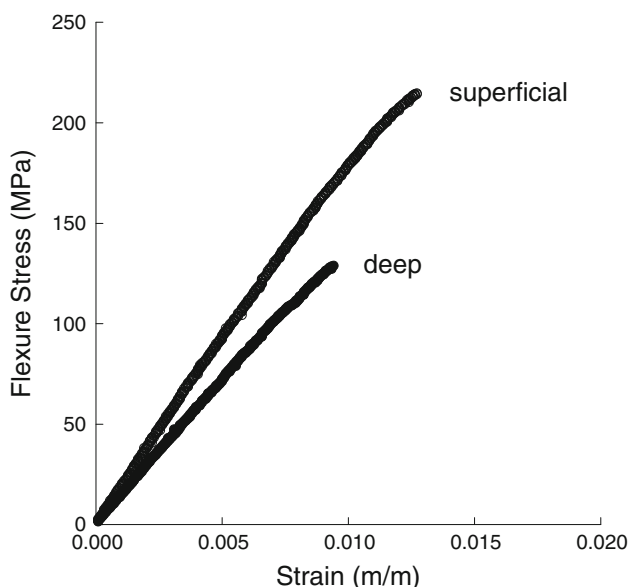


**Fig. 2** Representative stress–strain diagrams obtained from results of the flexure tests for deep and superficial dentin

the Weibull parameters for properties of the beams with and without flaws. In general, the Weibull moduli for the deep dentin were lower than those values determined for the superficial dentin. Characteristic values for the properties are essentially equivalent to the median value, and are ranked consistently with the average properties listed in Table 1. Again, results for the deep dentin were significantly lower than the corresponding values for the superficial dentin.

All of the dentin beams failed within the region of maximum normal stress between the two interior pin supports. In beams with surface flaw, fracture appeared to initiate from the indent in only two of the 40 beams, both of which were superficial dentin. An evaluation of the fracture surfaces showed that failure initiated from the tensile side, and that the beams of deep and superficial dentin exhibited similar, but distinct features. Fracture surfaces of the superficial dentin (Fig. 4a) were parallel to the dentin tubules on the tensile side of the neutral axis, and exhibited a prominent compression curl near the compressive surface. Fracture surfaces of the deep dentin beams (Fig. 4b) showed similar features on the tensile side, but far smaller compression curl. In fact, a compression curl was not evident on many beams of deep dentin. For these beams fracture occurred exclusively along the plane of maximum normal stress.

Representative FTIR-RM maps of the mineral to collagen ratio and relative collagen content are shown in Fig. 5a and b, respectively. Note that the selected contrast range was chosen to highlight the distribution for dentin and as such, the high mineral to collagen ratio of the enamel is out of range. There are quantitative differences evident in the relative presence of mineral and collagen over the crown, and in comparison of the crown and root. Most evident are the increase in the mineral to collagen ratio and the decrease in relative collagen content from the DEJ towards the pulp along the intercuspal path. The average ratios of mineral to collagen content within the cuspal and intercuspal regions and at the three locations of evaluation (deep, middle and superficial) are shown in Fig. 6a. Similarly, the relative collagen content at these locations is shown in Fig. 6b. Note that the chemical composition of superficial dentin in the intercuspal region is significantly different ( $P < 0.05$ ) than at all of the other locations examined. Specifically, the superficial dentin exhibited significantly lower mineral to collagen ratio, and significantly greater relative collagen content.

### 4 Discussion

Results of the flexure experiments showed that there are significant differences between the mechanical behavior of deep and superficial dentin. All of the mechanical

**Table 1** Mechanical properties of the dentin specimens

Group	Elastic modulus (GPa)	<i>P</i>	Strength (MPa)	<i>P</i>	Strain (m/m)	<i>P</i>	Energy (MPa)	<i>P</i>
Control deep superficial	13.4 (2.2)	0.01	119 (31)	0.005	0.008 (0.003)	0.005	0.64 (0.33)	0.001
	14.8 (2.2)		169 (28)		0.011 (0.002)		1.15 (0.42)	
W/Indent deep superficial	14.5 (2.9)	0.01	113 (22)	0.0001	0.008 (0.002)	0.001	0.57 (0.17)	0.0001
	16.7 (2.8)		171 (31)		0.011 (0.002)		1.21 (0.60)	
All deep superficial	14.0 (2.6)	0.05	116 (27)	0.0001	0.008 (0.002)	0.0001	0.60 (0.26)	0.0001
	15.8 (2.6)		170 (29)		0.011 (0.002)		1.18 (0.50)	

All values are listed in terms of the average and (standard deviation)

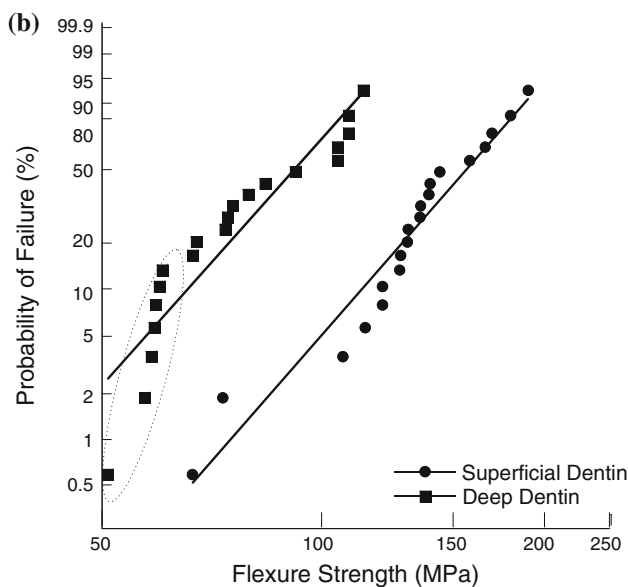
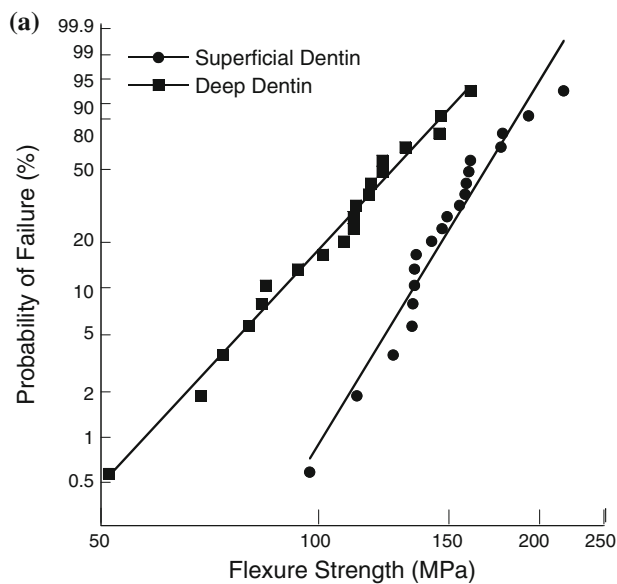


**Fig. 3** Weibull distributions for the flexure strength of the dentin beams. **a** Specimen from superficial dentin **b** specimen from deep dentin. Note the tail in the failure distribution of the deep dentin

**Table 2** Weibull parameters for the mechanical properties of inner and outer dentin

Group	Strength		Strain to fracture		Energy to fracture	
	<i>m</i> <sup>a</sup> LSE:MLE	<i>C</i> <sup>b</sup> (MPa)	<i>m</i> <sup>a</sup> LSE:MLE	<i>C</i> <sup>b</sup>	<i>m</i> <sup>a</sup> LSE:MLE	<i>C</i> <sup>b</sup> (MPa)
Superficial						
Control	4.90:7.37	178	6.13:6.82	0.012	2.50:3.39	1.3
W/indent	5.37:5.61	194	5.32:5.02	0.012	2.76:2.40	1.38
Deep						
Control	3.57:3.83	135	3.79:3.35	0.009	1.86:1.81	0.67
W/indent	4.12:4.78	121	4.32:4.80	0.009	2.14:2.28	0.57

There were no significant differences between the responses for beams with and without indent

<sup>a</sup> LSE and MLE refer to estimates obtained using least squares error and maximum likelihood estimation

<sup>b</sup> Obtained using LSE

properties were depth-dependent, which is consistent with results of earlier studies that examined the spatial-dependence in mechanical behavior of dentin. Previous studies have reported that deep dentin exhibits significantly lower hardness [23–25], lower ultimate tensile strength [13, 26–28] and lower shear strength [29, 30]. The results for critical strain and energy to fracture presented in Table 1 are unique contributions and have not been previously reported. Both of these properties exhibited significant differences between the two regions; the superficial dentin exhibited a 30% larger critical strain and over 100% larger energy to fracture. Earlier studies on the mechanical behavior of coronal dentin have suggested that dentin failure is governed by a critical strain rather than a critical stress criterion [13, 31]. Results of the flexure experiments distinguish that the strain to fracture of dentin is depth-dependent and that deep dentin exhibits a lower critical strain (Table 1). Therefore, deep dentin is more brittle than superficial dentin, which is consistent with expected behavior according to the larger mineral to collagen ratio.

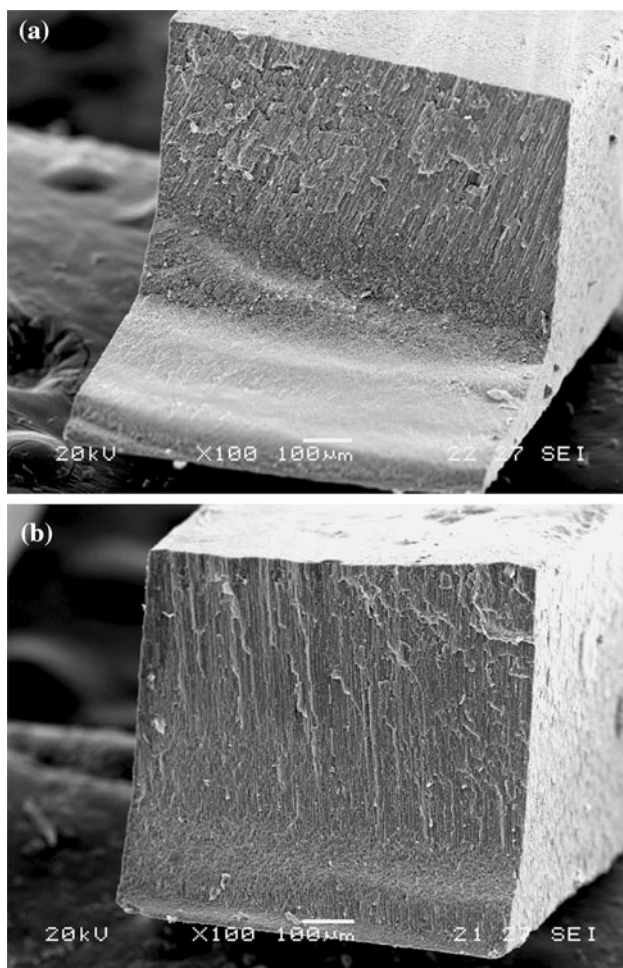
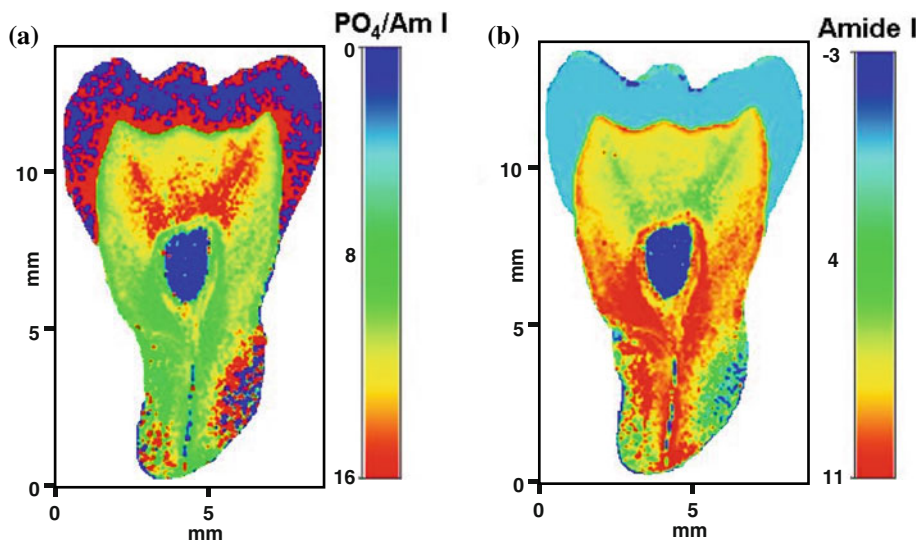


**Fig. 4** Typical fracture surfaces of selected dentin specimens. Neither of the specimens had a surface flaw introduced using indentation. Note the comparatively large compression curl evident on the bottom of the superficial dentin beam in (a). **b** specimen from deep dentin

Results for the flexure strength followed a Weibull distribution, which is consistent with those of Staninec et al. [13] for the ultimate tensile strength (UTS) of coronal dentin. There the maximum likelihood estimates for the Weibull modulus ranged from 3.15 to 6.00. While these values are consistent with the range in Weibull moduli for the strength and strain to fracture in Table 2, there are important differences between these studies. A correction is required to perform a direct comparison of the Weibull modulus according to the mode of loading (i.e. tension vs bending). Also, the maximum normal stress in the aforementioned evaluation [13] was oriented parallel to the dentin tubules, which is perpendicular to the orientation used in the flexural test. Tubule orientation contributes to the apparent tensile strength of dentin [26, 27, 32], with the lowest strength resulting from conditions of maximum normal stress aligned with the tubules. Despite these differences, there is general consistency in the Weibull moduli between these studies, which suggests that the distribution in flaw sizes is similar and they played an equivalent role in the failure process. Perhaps most important, both evaluations were performed using coronal dentin of 3rd molars, which were likely engaged in limited to no masticatory loading. The dentin of teeth undergoing more extensive oral activity could exhibit different flaw sizes/populations that contribute to the mechanical property distributions. This is an important concern and should be considered in future studies.

The indentation surface flaws had no noticeable effect on the average flexure strength (Table 1) or the strength distribution of the dentin beams (Fig. 3). Therefore, in both regions of evaluation the intrinsic flaws were more critical than the stress concentration posed by the indents. It is important to highlight that while the stress concentration

**Fig. 5** Typical maps of the mineral to collagen ratio and the relative collagen content obtained from FTIR microspectroscopy. The maps were obtained from scans of a 3rd molar from a 23 year old patient. Note that the maps do not provide detailed information for the enamel as the contrast range has been optimized for the dentin. *Light/Blue* regions represent the lowest intensity and *dark/red* regions represent the highest. **a** Mineral to collagen ratio. **b** Relative collagen content (Color figure online)



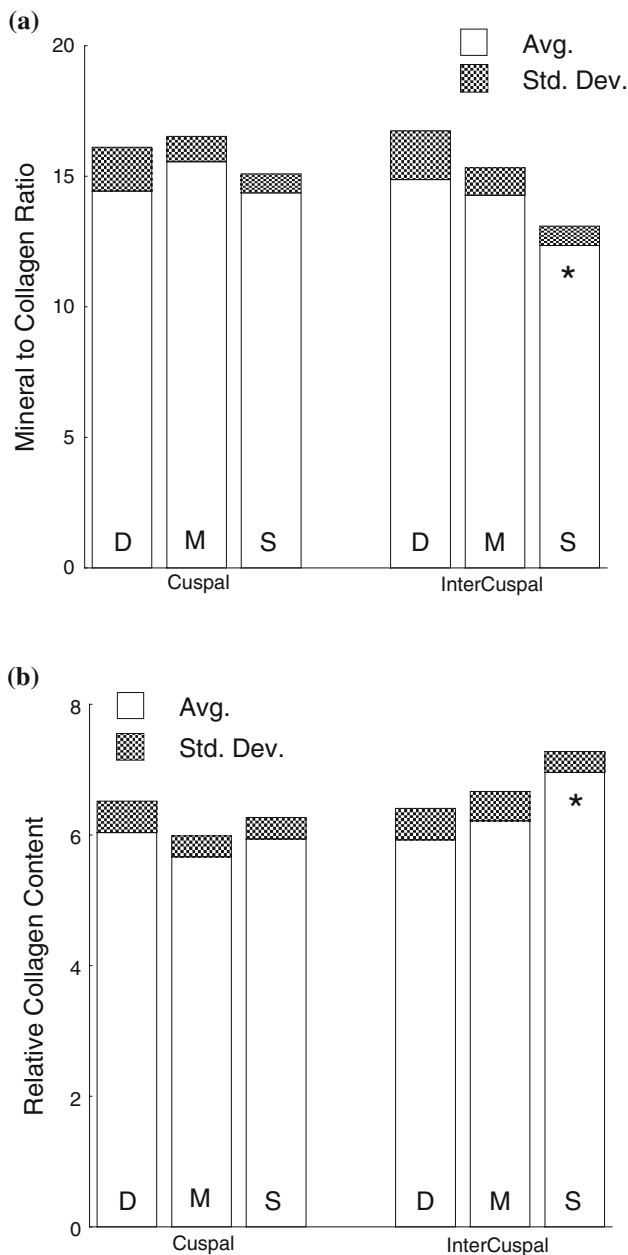


**Fig. 6** Results of the FTIR-RM analysis for the coronal dentin. Note that the relative measures of mineral to collagen ratio and collagen content for the cuspal region are the average of both cusps. Columns indicated with \* are significantly different ( $P < 0.05$ ). **a** mineral to collagen ratio, **b** relative collagen content

posed by the indent was approximately 1.75 [17], the small notch radius of the indent resulted in a very localized region of elevated stress. Results for the deep dentin showed the smallest Weibull moduli (Table 2), suggesting that the tissue within this region exhibited a larger flaw size distribution [33]. That could arise from the larger tubule diameters in deep dentin, or the semblance of larger flaws that are actually small groups of tightly packed tubules. The moduli obtained for dentin are comparable to those

reported for the bond strengths of bonding agents (avg = 4.84; range: 2.52 to 7.82) [34], and larger than those characterizing the distribution in strengths between dentin and resin composites (avg = 2.84; range: 1.67 to 4.99) [35]. These findings suggest that flaws associated with the adhesive interface (dentin/resin) play an equivalent role in the strength variations as intrinsic flaws within the supporting tissue substrate (i.e. dentin). There are limitations to this interpretation. Results of both the present and past evaluations have characterized the dentin from teeth that experienced limited oral function, and aside from the single surface flaws, the dentin beams were nominally flaw free. They did not possess near-surface defects typical of those that may be introduced during the cavity preparation [36, 37].

In past studies of dentin the differences in properties with depth have been primarily attributed to the tubule density. Pashley et al. [23] correlated the decrease in dentin microhardness from the DEJ towards the pulp with the increase in tubule density. There the reduction in hardness was believed to be largely due to the increase in tubule diameter and the reduction in intertubular dentin. The changes in tubule density have also been identified in the spatial variations in tensile strength. Deep coronal dentin has been shown to be weaker than superficial dentin and the differences attributed to tubule density [26, 27]. Similar dependence of strength on tubule density has been identified in the root [38]. As a result of the increase in tubule diameter near the pulp, the cross-section area occupied by the tubules increases by approximately 20% [39]. That reduction in “load-bearing” material would result in an equivalent reduction in strength (of 20%). But results from the flexural tests (Table 1) and earlier measures of the tensile strength [25–27] show that there is nearly a 50% reduction in strength between deep and superficial dentin. That difference cannot be explained by the changes in tubule density and area fraction alone. Results from the FTIR-RM evaluations showed that within the intercuspal region there was approximately 20% increase in the mineral collagen ratio (Fig. 6a) and over 15% decrease in the relative collagen content (Fig. 6b) from the superficial dentin towards the interior. These changes in the chemical composition cause an increase in apparent brittleness of the tissue and reduction in damage tolerance. Consequently, though the reduction in strength and energy to fracture with depth (Table 1) may be partly attributed to the lumen dimensions, it is also caused by the larger apparent flaw sensitivity that stems from the gradient in chemical composition. Contributions from spatial differences in the degree of collagen cross-linking density [40] remain to be addressed.

Although results of this investigation provide further understanding of the spatial variations in mechanical

behavior of coronal dentin and the importance of microstructure, there are remaining concerns. Dentin is susceptible to fatigue failure [8, 9] and flaws generally play the largest role in the failure of materials subjected to cyclic loading. The larger flaw size distribution and greater mineral to collagen ratio of deep dentin suggests that the fatigue properties will vary with depth as well. Of additional concern, the region with the lowest resistance to fracture and largest contribution of flaws was that with the highest mineral to collagen ratio. The largest ratios were located beneath the cusps (Fig. 5). Unfortunately, the flexure specimen geometry limited the evaluation to properties of dentin within the intercuspal region only. Physiological processes that cause equivalent changes in the mineral to collagen ratio could also be important. There is a reduction in average lumen diameter with patient age, which results in an overall increase in the mineral content of dentin. And there is a significant reduction in strength of human dentin with patient age under both static and cyclic loading [10, 41, 42]. Results of the present investigation suggest indirectly that the reduction in strength of dentin with age could partly be attributed to an increase in flaw sensitivity of the tissue and change in the population of intrinsic flaws. Alternatively, there could be compounding influence from changes in moisture content, which also contribute to the degree of apparent brittleness of dentin [43]. Those aspects of mechanical behavior are clinically relevant and may contribute to the nature of restoration failures in the elderly. Investigations are presently underway to address these issues.

## 5 Conclusions

An experimental investigation was performed to evaluate the mechanical behavior of coronal dentin at different depths relative to the Dentin Enamel Junction (DEJ), and to assess the importance of microstructure, chemical composition and apparent flaw sensitivity. Based on results of the investigation the following conclusions were drawn:

(1) The deep dentin exhibited a significantly lower elastic modulus ( $P \leq 0.05$ ), strength ( $P \leq 0.005$ ), critical strain ( $P \leq 0.005$ ) and energy to fracture ( $P \leq 0.001$ ) than those properties of the superficial dentin. There were no significant differences in the properties of the beams with and without indentation surface flaws.

(2) The mechanical properties associated with failure of both deep and superficial dentin followed a Weibull probability distribution. Properties for the deep dentin exhibited lower Weibull moduli, which suggests that the tissue in this region possesses a greater flaw size distribution.

(3) The intercuspal superficial dentin exhibited a significantly lower mineral to collagen ratio ( $P \leq 0.05$ ) and

significantly higher collagen content ( $P \leq 0.02$ ) than the deep dentin. The region with lowest mineral to collagen ratio (superficial dentin) exhibited the highest strength, critical strain and energy to fracture.

**Acknowledgments** This research was supported in part by an award from the National Institutes of Health (NIDCR DE016904) and the National Science Foundation (BES 0238237). Aftin Ross, Heon Ryou and Nikhil Amin were undergraduate students during the course of the research and Ms Ross acknowledges support from the MARC U-STAR program.

## References

1. Marshall DB, Evans AG, Khuri Yakub BT, Tien JW, Kino GS. Nature of machining damage in brittle materials. *Proc Roy Soc Lond Ser A Math Phys Sci.* 1983;385(1789):461–75.
2. Xu HHK, Padture NP, Jahanmir S. Effect of microstructure on material-removal mechanisms and damage tolerance in abrasive machining of silicon carbide. *J Am Cer Soc.* 1995;78(9):2443–8.
3. Quinn GD, Ives LK, Jahanmir S. On the nature of machining cracks in ground ceramics. Part I: SRBSN strengths and fractographic analysis. *Mach Sci Technol.* 2005;9(2):169–210.
4. Quinn GD, Ives LK, Jahanmir S. On the nature of machining cracks in ground ceramics: part II, comparison to other silicon nitrides and damage maps. *Mach Sci Technol.* 2005;9(2):211–37.
5. Sehy C, Drummond JL. Micro-cracking of tooth structure. *Am J Dent.* 2004;17(5):378–80.
6. Yan J, Taskonak B, Mecholsky JJ. Fractography and fracture toughness of human dentin. *J Mech Behav Biomed Mater.* 2009; 2(5):478–84.
7. Staninec M, Meshkin N, Manesh SK, Ritchie RO, Fried D. Weakening of dentin from cracks resulting from laser irradiation. *Dent Mater.* 2009;25(4):520–5.
8. Nalla RK, Imbeni V, Kinney JH, Staninec M, Marshall SJ, Ritchie RO. In vitro fatigue behavior of human dentin with implications for life prediction. *J Biomed Mater Res.* 2003;66(1): 10–20.
9. Arola D, Reprogl R. Tubule orientation and the fatigue strength of human dentin. *Biomaterials.* 2006;27(9):2131–40.
10. Arola D, Reprogl R. Effects of aging on the mechanical behavior of human dentin. *Biomaterials.* 2005;26(18):4051–61.
11. Arola D, Huang MP, Sultan MB. The failure of amalgam restorations due to cyclic fatigue crack growth. *J Mat Sci Mater Med.* 1999;10(6):319–27.
12. Bajaj D, Sundaram N, Arola D. An examination of fatigue striations in human dentin: in vitro and in vivo. *J Biomed Mater Res Appl Biomater.* 2008;85(1):149–59.
13. Staninec M, Marshall GW, Hilton JF, Pashley DH, Gansky SA, Marshall SJ, Kinney JH. Ultimate tensile strength of dentin: evidence for a damage mechanics approach to dentin failure. *J Biomed Mater Res.* 2002;63(3):342–5.
14. Kinney JH, Marshall SJ, Marshall GW. The mechanical properties of human dentin: a critical review and re-evaluation of the dental literature. *Crit Rev Oral Biol Med.* 2003;14(1):13–29.
15. ISO Standard 18756 (2003) Fine ceramics (advanced ceramics, advanced technical ceramics)-determination of fracture toughness of monolithic ceramics at room temperature by the surface crack in flexure (SCF) method.
16. Scherrer SS, Kelly JR, Quinn GD, Xu K. Fracture toughness (K<sub>Ic</sub>) of a dental porcelain determined by fractographic analysis. *Dent Mater.* 1999;15(5):342–8.



17. Peterson RE. Stress concentration factors. New York: Wiley; 1974.
18. Weibull W. A statistical distribution function of wide applicability. *J Appl Mech.* 1951;18:293–7.
19. Davies IJ. Best estimate of Weibull modulus obtained using linear least squares analysis: an improved empirical correction factor. *J Mat Sci.* 2004;39(4):1441–4.
20. Tesch W, Eidelman N, Roschger P, Goldenberg F, Klaushofer K, Fratzl P. Graded microstructure and mechanical properties of human crown dentin. *Calcif Tissue Int.* 2001;69(3):147–57.
21. Eidelman N, Simon CG. Characterization of combinatorial polymer blend composition gradients by FTIR Microspectroscopy. *J Res Natl Inst Stand Technol.* 2004;109(2):219–31.
22. Chalmers JM, Everall NJ, Ellison S. Specular reflectance: a convenient tool for polymer characterisation by FTIR-microscopy? *Micron.* 1996;27(5):315–28.
23. Pashley D, Okabe A, Parham P. The relationship between dentin microhardness and tubule density. *Endod Dent Traumatol.* 1985; 1(5):176–9.
24. Kinney JH, Balooch M, Marshall SJ, Marshall GW Jr, Weihs TP. Atomic force microscope measurements of the hardness and elasticity of peritubular and intertubular human dentin. *J Biomech Eng.* 1996;118(1):133–5.
25. Fuentes V, Toledano M, Osorio R, Carvalho RM. Microhardness of superficial and deep sound human dentin. *J Biomed Mater Res A.* 2003;66(4):850–3.
26. Carvalho RM, Fernandes CA, Villanueva R, Wang L, Pashley DH. Tensile strength of human dentin as a function of tubule orientation and density. *J Adhes Dent.* 2001;3(4):309–14.
27. Inoue S, Pereira PN, Kawamoto C, Nakajima M, Koshiro K, Tagami J, Carvalho RM, Pashley DH, Sano H. Effect of depth and tubule direction on ultimate tensile strength of human coronal dentin. *Dent Mater J.* 2003;22(1):39–47.
28. Giannini M, Soares CJ, de Carvalho RM. Ultimate tensile strength of tooth structures. *Dent Mater.* 2004;20(4):322–9.
29. Konishi N, Watanabe LG, Hilton JF, Marshall GW, Marshall SJ, Staninec M. Dentin shear strength: effect of distance from the pulp. *Dent Mater.* 2002;18(7):516–20.
30. Watanabe LG, Marshall GW Jr, Marshall SJ. Dentin shear strength: effects of tubule orientation and intratooth location. *Dent Mater.* 1996;12(2):109–15.
31. Nalla RK, Kinney JH, Ritchie RO. On the fracture of human dentin: is it stress- or strain-controlled? *J Biomed Mater Res A.* 2003;67(2):484–95.
32. Lertchirakarn V, Palamara JE, Messer HH. Anisotropy of tensile strength of root dentin. *J Dent Res.* 2001;80(2):453–6.
33. Trustrum K, Jayatilaka ADe-S. Applicability of Weibull analysis for brittle materials. *J Mat Sci.* 1983;18(9):2765–70.
34. Dickens SH, Cho BH. Interpretation of bond failure through conversion and residual solvent measurements and Weibull analyses of flexural and microtensile bond strengths of bonding agents. *Dent Mater.* 2005;21(4):354–64.
35. Burrow MF, Thomas D, Swain MV, Tyas MJ. Analysis of tensile bond strengths using Weibull statistics. *Biomaterials.* 2004; 25(20):5031–5.
36. Xu HHK, Kelly JR, Jahanmir S, Thompson VP, Rekow ED. Enamel subsurface damage due to tooth preparation with diamonds. *J Dent Res.* 1997;76(10):1698–706.
37. Banerjee A, Kidd EA, Watson TF. Scanning electron microscopic observations of human dentine after mechanical caries excavation. *J Dent.* 2000;28(3):179–86.
38. Mannocci F, Pilecki P, Bertelli E, Watson TF. Density of dentinal tubules affects the tensile strength of root dentin. *Dent Mater.* 2004;20(3):293–6.
39. Pashley DH. Smear layer: physiological considerations. *Oper Dent.* 1984;suppl 3:13–29.
40. Miguez PA, Pereira PN, Atsawasuwan P, Yamauchi M. Collagen cross-linking and ultimate tensile strength in dentin. *J Dent Res.* 2004;83(10):807–10.
41. Kinney JH, Nalla RK, Pople JA, Breunig TM, Ritchie RO. Age-related transparent root dentin: mineral concentration, crystallite size, and mechanical properties. *Biomaterials.* 2005;26(16): 3363–76.
42. Arola D, Bajaj D, Ivancik J, Majd H, Zhang D. Fatigue of biomaterials: hard tissues. *Int J Fat.* 2010;32(9):1400–12.
43. Jameson MW, Hood JA, Tidmarsh BG. The effects of dehydration and rehydration on some mechanical properties of human dentine. *J Biomech.* 1993;26(9):1055–65.